# Supplement for: Longer heat pulses disrupt bacterial communities by decoupling resistance from recovery.

Authors: Ana-Hermina Ghenu, Anjaney J. Pandey, Zachary M. Bailey, David R. Johnson, and Madhav P. Thakur

Materials & Methods

**Table S1: List of bacterial strains used in the experiment.**

ID	Strain identification	Isolated from…	Fluorescence	Lab of Origin & Strain ID in their Collection	Ref.
BSC001	*Pseudomonas putida F1*	creek	sYFP	Jan van der Meer (UniL, CH) 7609	--
BSC002	*Pseudomonas putida KT2440*	?	mScarlet	Jan van der Meer (UniL, CH) 7598	--
BSC003	*Pseudomonas putida uwc 2*	soil	mTagBFP2	Jan van der Meer (UniL, CH) 7597	--
BSC004	*Pseudomonas veronii*	?	mTagBFP2	Jan van der Meer (UniL, CH) 7591	--
BSC005	*Pseudomonas veronii*	?	mScarlet	Jan van der Meer (UniL, CH) 7592	--
BSC006	*Pseudomonas veronii*	?	mCherry	Jan van der Meer (UniL, CH) 3434	--
BSC007	*Pseudomonas knackmussii B13*	soil	mCherry	Jan van der Meer (UniL, CH) 2586	--
BSC008	*Pseudomonas knackmussii B14*	sewage	eGFP	Jan van der Meer (UniL, CH) 1369	--
BSC009	*Pseudomonas plecoglossicida*	soil	*N/A*	Antonis Chatzinotas (UFZ, DE) B405	[30]
BSC010	*Pseudomonas putida mt-2 KT2440*	soil	*N/A*	Antonis Chatzinotas (UFZ, DE) B410	--
BSC015	*Pseudomonas putida KT2440*	?	GFP	Pilar Junier (UniNe, CH)	--
BSC019	*Pseudomonas grimontii*	soil	*N/A*	Jan van der Meer (UniL, CH) 906 (SV16)	[31]
CK101	*Pseudomonas protegens Pf5*	soil	mTourquoise2	Christof Keel (UniL, CH) Pf5-*mtou*	[32]
CK102	*Pseudomonas protegens Pf5*	soil	mCherry	Christof Keel (UniL, CH) Pf5-*mche*	[33]
CK103	*Pseudomonas protegens CHAO*	soil	sGFP2	Christof Keel (UniL, CH) CHA0-*gfp2*	[34]
CK104	*Pseudomonas protegens CHAO*	soil	mCherry	Christof Keel (UniL, CH) CHA0-*mche*	[34]
BSC028	*Pseudomonas grimontii*	*(see above)*	sGFP2	**BSC019**	This.
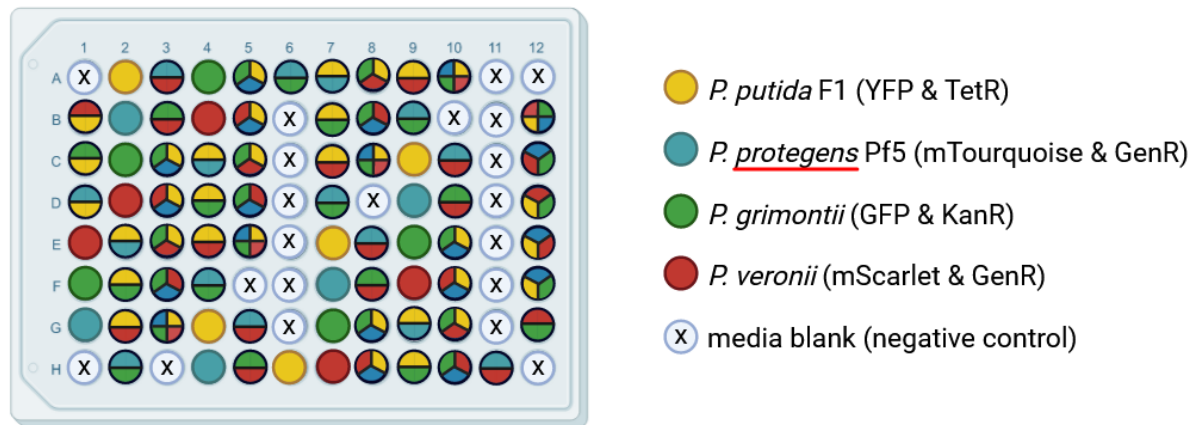
Figure S1. The arrangement of the 15 communities (n=5) on the 96-well microplates during Experiment II. Communities are arranged in five blocks across the microplate such that two of the blocks are all edge wells and the other three blocks are all non-edge wells. Coloured circles represent communities inoculated with the species indicated in the legend. Media blanks are shown with crosses. Figure created with BioRender.

Figure S2. Flow cytometry gating strategy to identify individual species. All events in the cells gate **(panel A)** are either assigned to species level, using a set of three nested polygon gates to identify events with single fluorophore expression **(panels B-E)**, or excluded from further analyses. For panels B-E), representative screenshots are taken from the FCS Express analysis for a positive sample (top plots) with all four species present and a negative sample (bottom plots) with the three other species present.
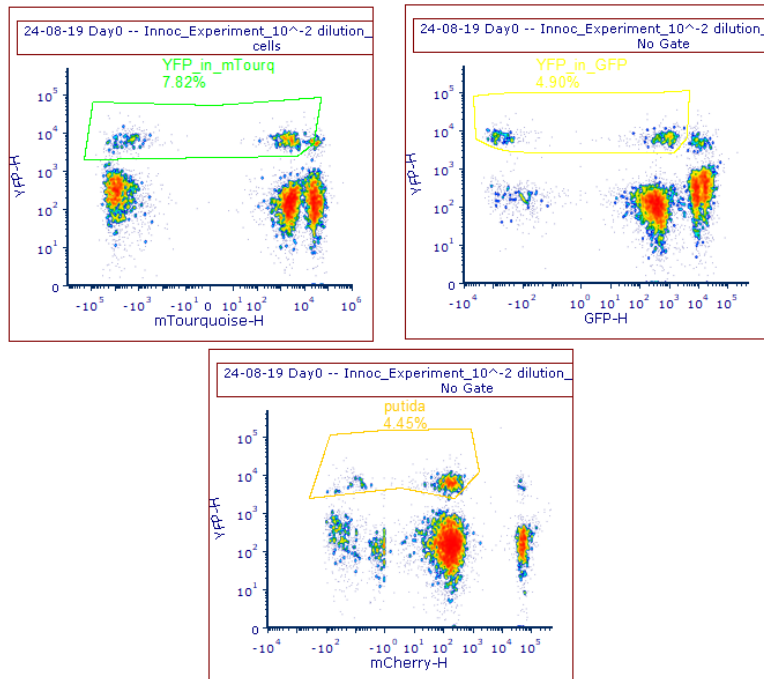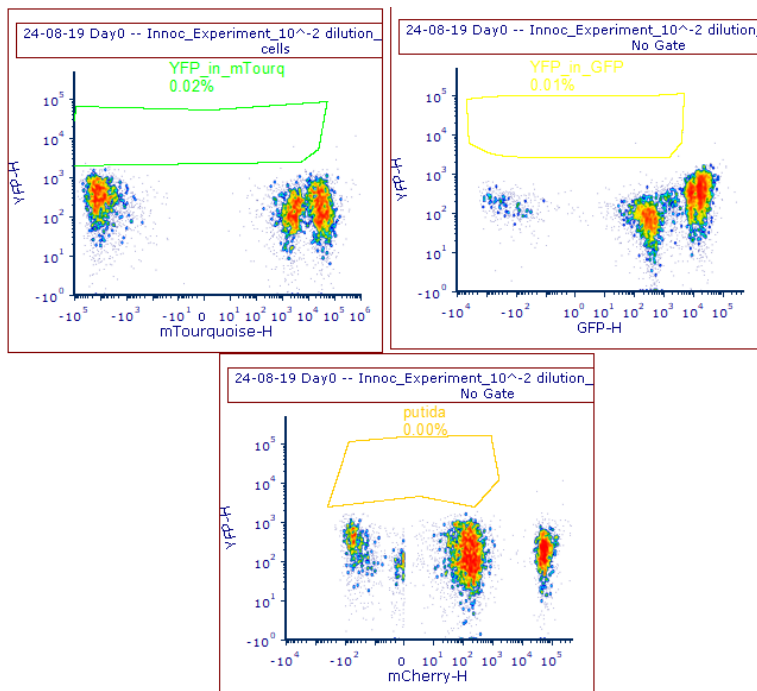
A)
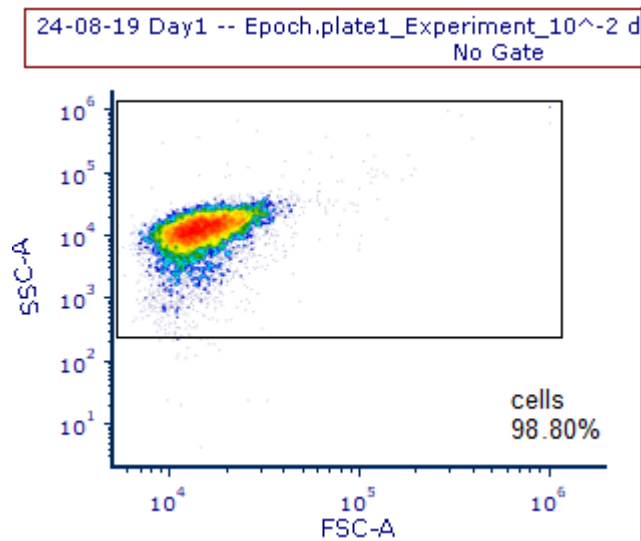
Figure S2 Panel A) A rectangular gate (black) in the forward scatter area (FSC-A) and side scatter area (SSC-A) was used to identify cells and exclude small particles, which are most likely debris.

B)

Gating strategy to identify the YFP-positive cell population (*P. putida)*:
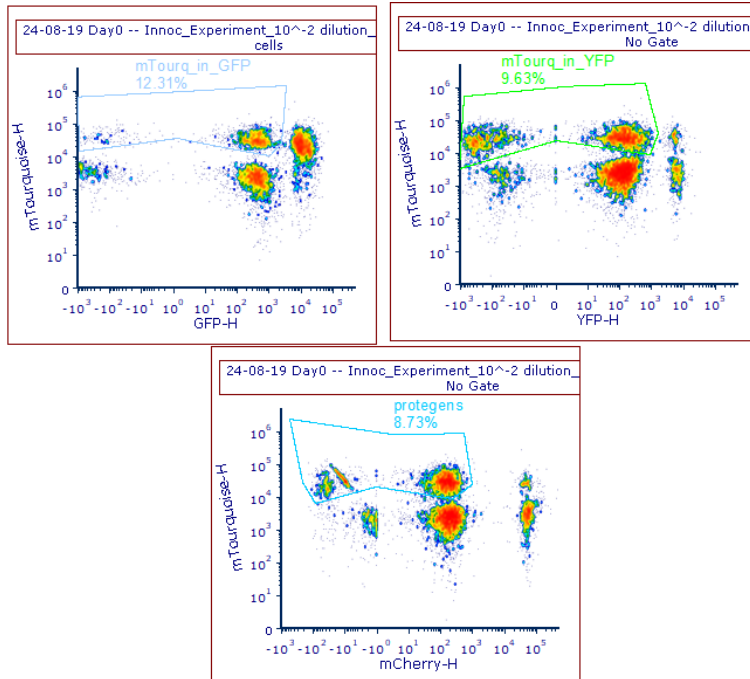

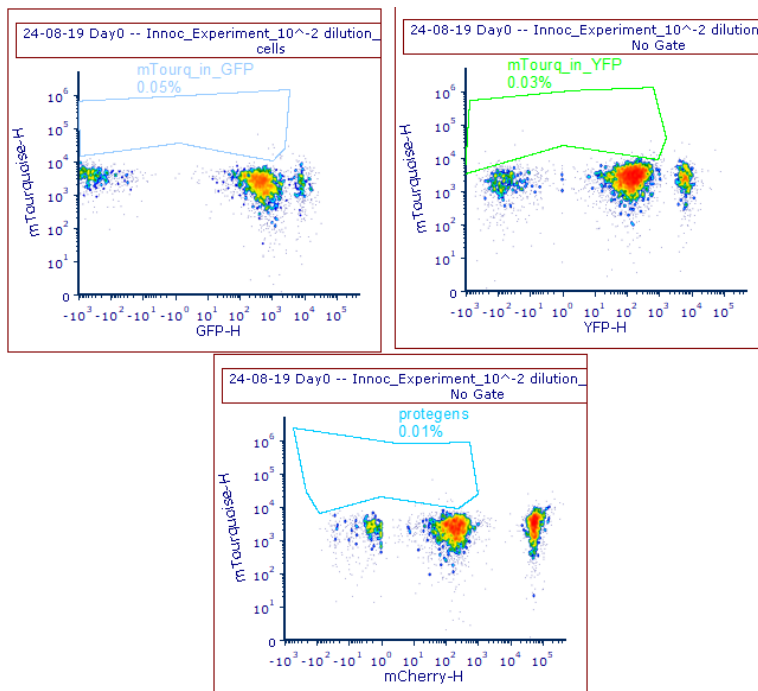The same strategy for a sample without *P. putida* (YFP-negative):

Figure S2 Panel B) Events from the cells gate are assigned to *P. putida* species because they express only YFP, as measured in YFP height (YFP-H, y-axis of all plots). First, mTourquoise events are excluded using a polygon gate in mTourquoise height (mTourquoise-H), then GFP events are excluded using a polygon gate in GFP height (GFP-H), and finally mCherry events are excluded using a polygon gate in mCherry height (mCherry-H).

C)

Gating strategy to identify the mTourquoise-positive cell population (*P. protegens)*:
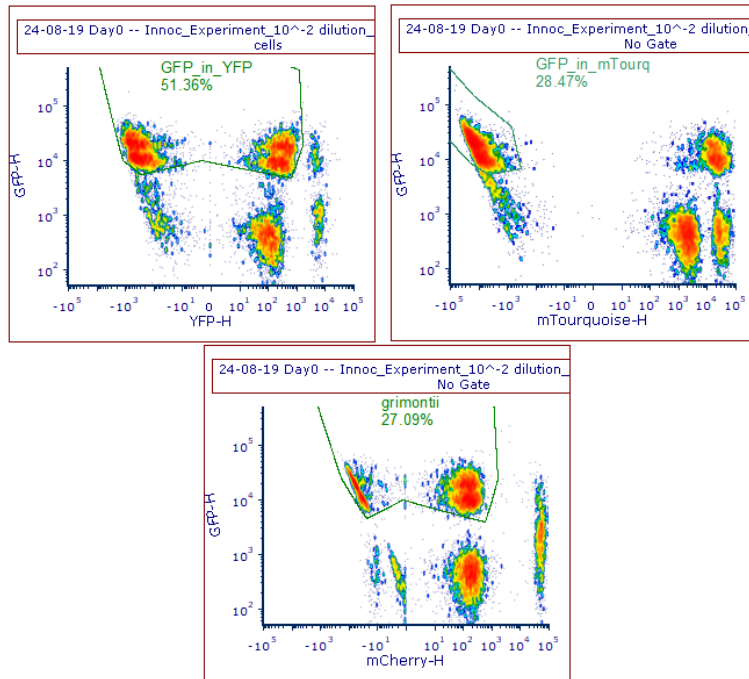

The same strategy for a sample without *P. protegens* (mTourquoise-negative):
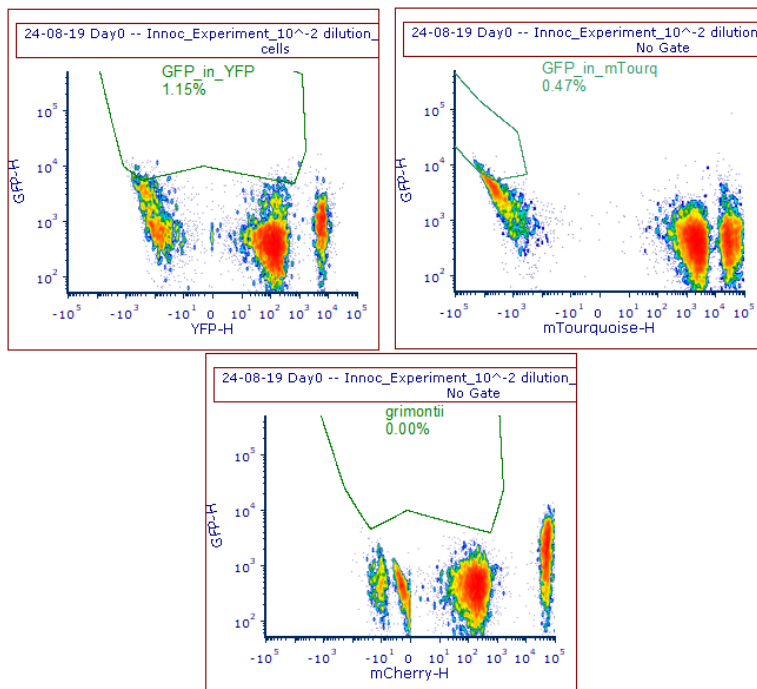

Figure S2 Panel C) Events from the cells gate are assigned to *P. protegens* species because they express only mTourquoise, as measured in mTourquoise height (mTourquoise-H, y-axis of all plots). First, GFP events are excluded using a polygon gate in GFP height (GFP-H), then YFP events are excluded using a polygon gate in YFP height (YFP-H), and finally mCherry events are excluded using a polygon gate in mCherry height (mCherry-H).

D)

Gating strategy to identify the GFP-positive cell population (*P. grimontii*):
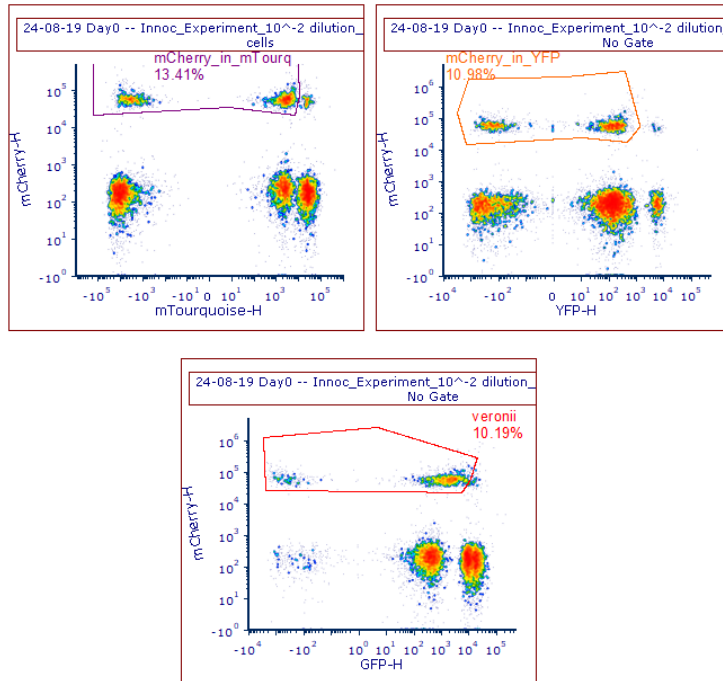

The same strategy for a sample without *P. grimontii* (GFP-negative):

Figure S2 Panel D) Events from the cells gate are assigned to *P. grimontii* species because they express only GFP, as measured in GFP height (GFP-H, y-axis of all plots). First, YFP events are excluded using a polygon gate in YFP height (YFP-H), then mTourquoise events are excluded using a polygon gate in mTourquoise height (mTourquoise-H), and finally mCherry events are excluded using a polygon gate in mCherry height (mCherry-H).

E)

Gating strategy to identify the mCherry-positive cell population (*P. veronii)*:

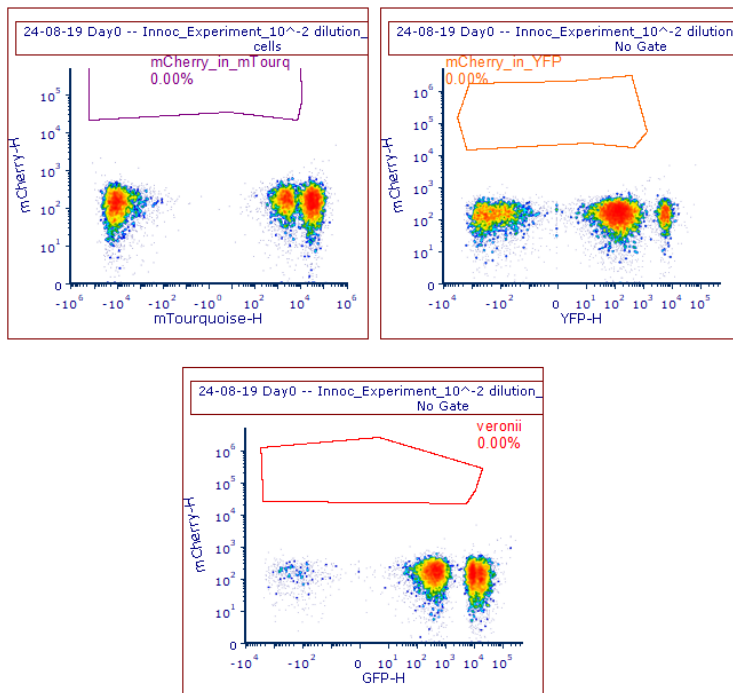The same strategy for a sample without *P. veronii* (mCherry-negative):

Figure S2 Panel E) Events from the cells gate are assigned to *P. veronii* species because they express only mCherry, as measured in mCherry height (mCherry-H, y-axis of all plots). First, mTourquoise events are excluded using a polygon gate in mTourquoise height (mTourquoise-H), then YFP events are excluded using a polygon gate in YFP height (YFP-H), and finally GFP events are excluded using a polygon gate in GFP height (GFP-H).
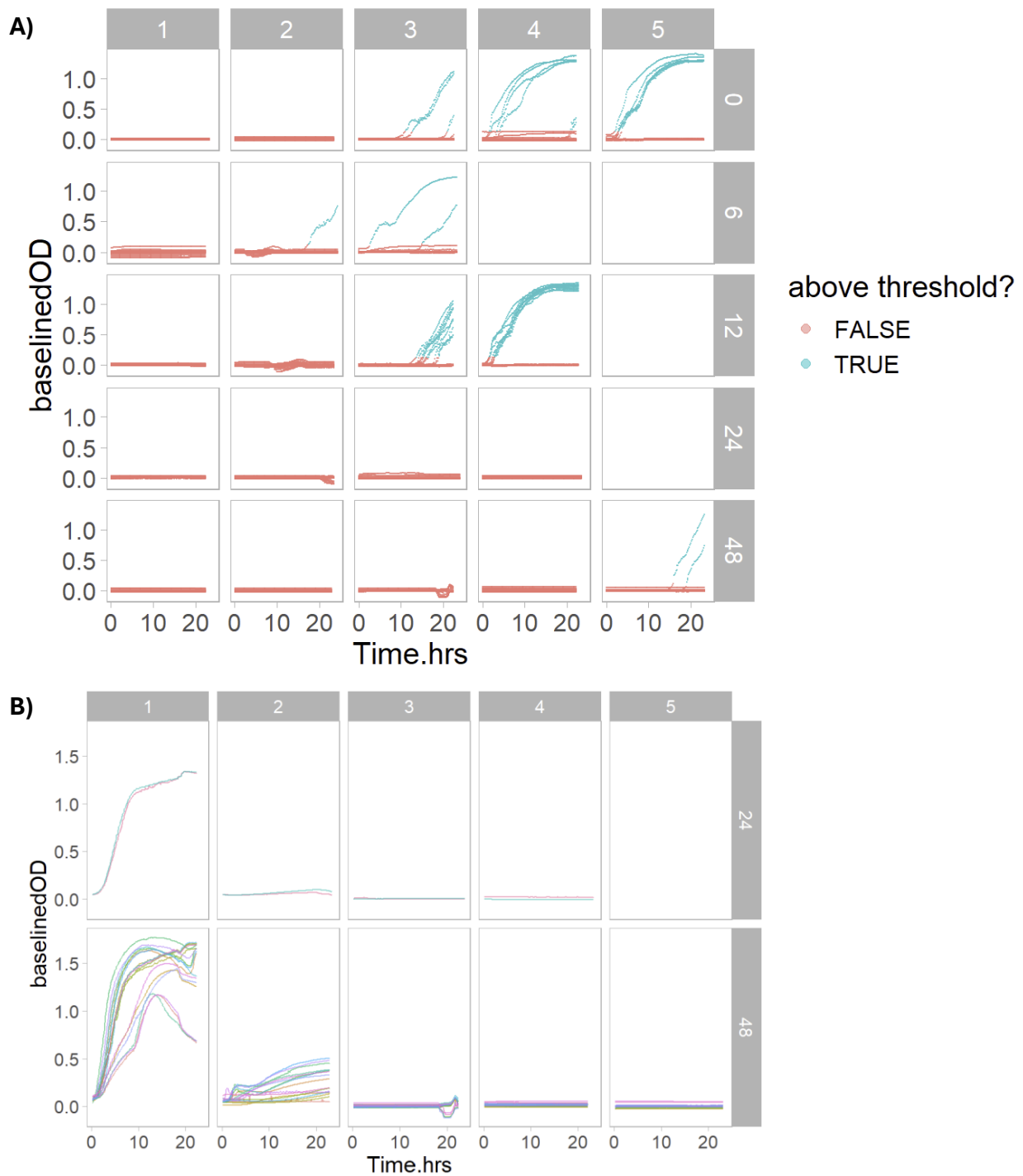
**Figure S3.** The same threshold was used for identifying contaminated well blanks (A) and wells that experienced community extinction (B). Different columns indicate the day of growth (Day 1 to 5) and different rows indicate the duration of the heat pulse treatment (0 indicates no heat control, 6 hrs heat, 12 hrs heat, 24 hrs heat, or 48 hrs heat) as illustrated in Figure 1 of the main text. There is no data for Days 4-5 of 6 hrs heat and Day 5 for 12 & 24 hrs heat (see main text). **A) Shows the baseline-subtracted OD for all well blanks, including contaminated well blanks.** Datapoints that are above the threshold are shown in blue and indicate contaminated blank wells. **B) Shows the baseline-subtracted OD only for non-blank communities that went extinct.** Datapoints are coloured by unique replicates.

Results for Experiment I
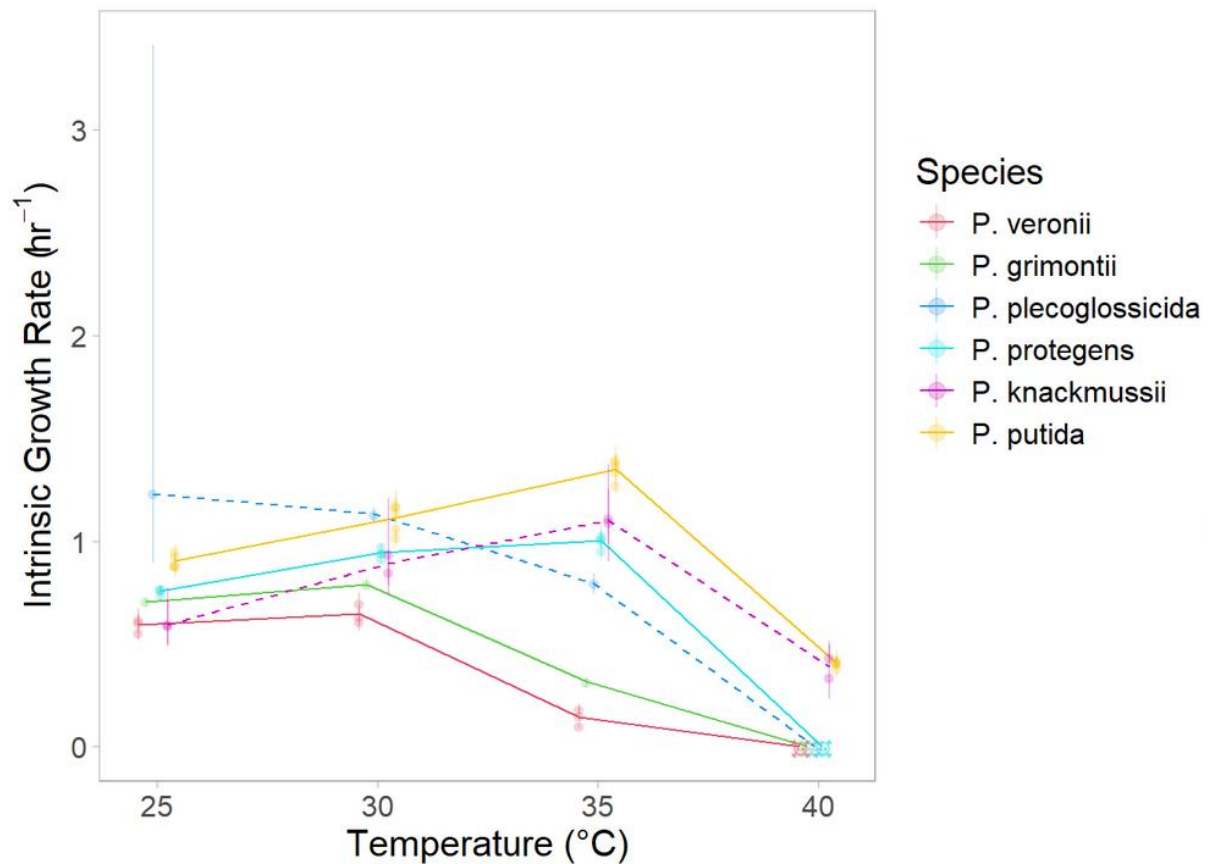
Figure S4. Net growth rate of stationary phase cultures as a function of temperature for 6 bacterial species in liquid media. Batch-culture intrinsic net growth rates (points) ± bootstrapped 95% confidence intervals (error bars) are shown for each strain inoculated from stationary phase. Temperatures without consistent growth after 48hrs are shown as skulls. Lines connect species averages, with solid lines indicating species with consistent rank across temperatures (used in Experiment II) and dashed lines indicating species that change rank across temperatures.
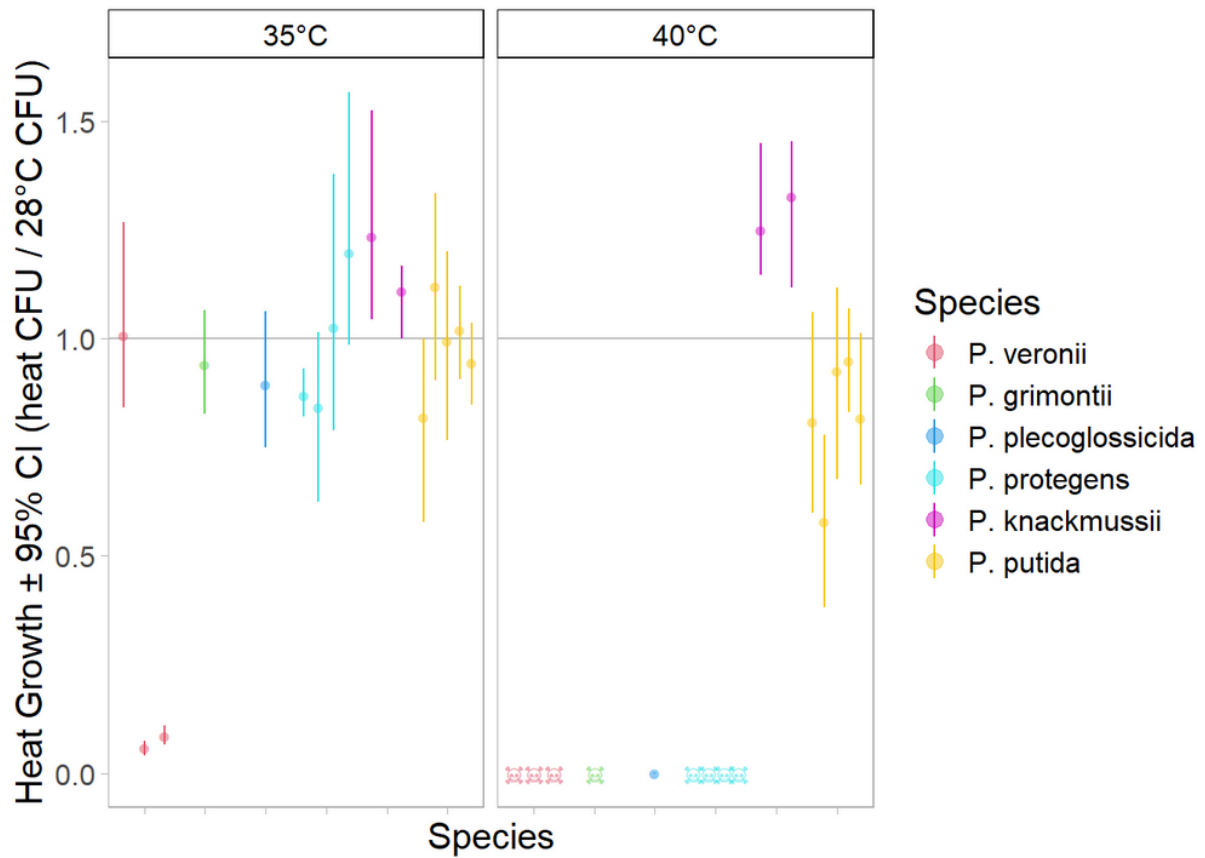
Figure S5. Relative growth of stationary phase cultures as a function of temperature for 6 bacterial species in solid media. CFUs at stress temperature as a fraction of CFUs at 28°C (dots) ± bootstrapped 95% confidence intervals (error bars) are shown for each strain inoculated from early exponential phase. Temperatures without any growth after 7 days are shown as skulls.
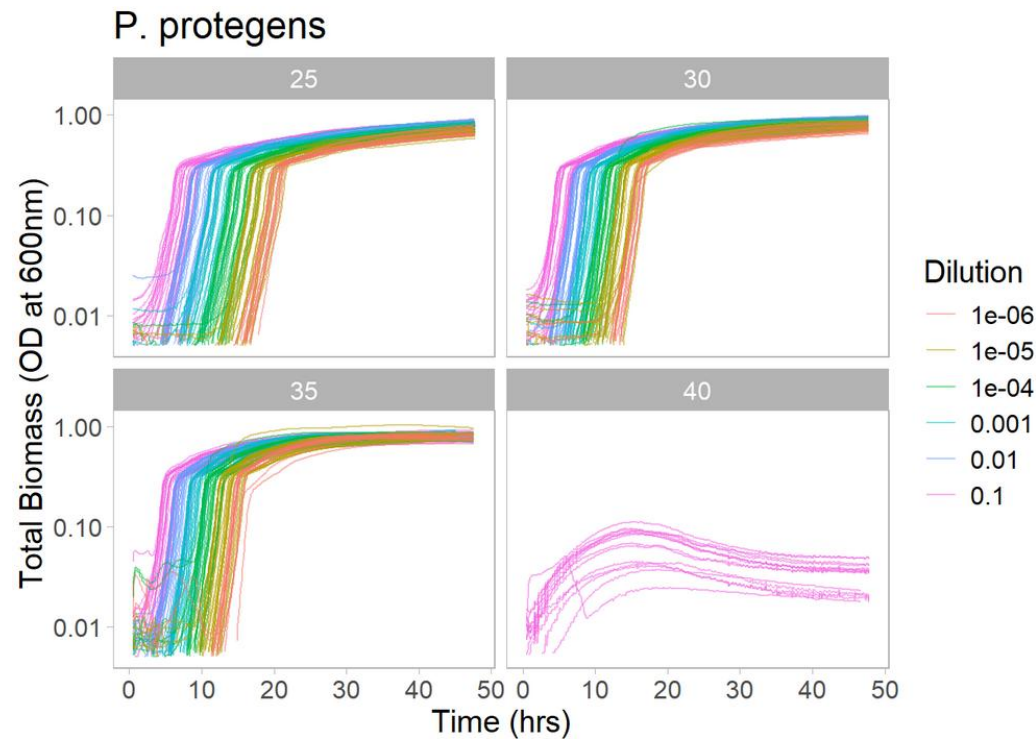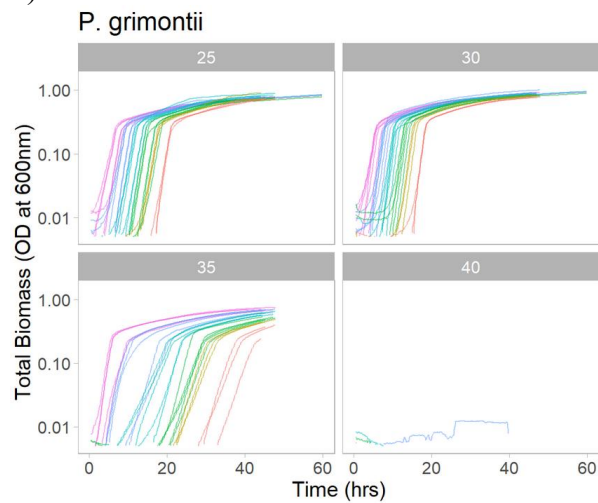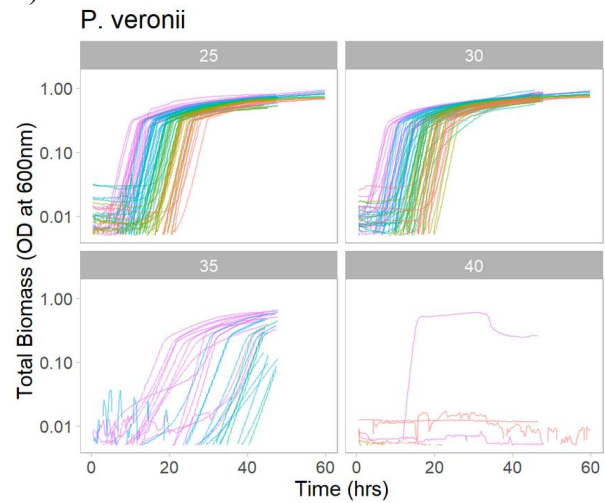
Figure S6. *P. protegens* **(a) exhibits density-dependence during growth at extreme heat, but other species that are also sensitive to extreme heat,** *P. grimontii* **(b) and** *P. veronii* **(c), do not show density-dependent growth.** Each panel shows the log of the OD (y-axis) over time (x-axis) for batch cultures inoculated, from both early exponential and stationary phase, at different starting dilutions (colours) that were incubated at different temperatures (facets). The most concentrated *P. protegens* cultures grew at about the same rate in the first five hours of growth at 40°C as when those was incubated at lower temperatures. However, there was a complete absence of growth at 40°C for all other starting concentrations.
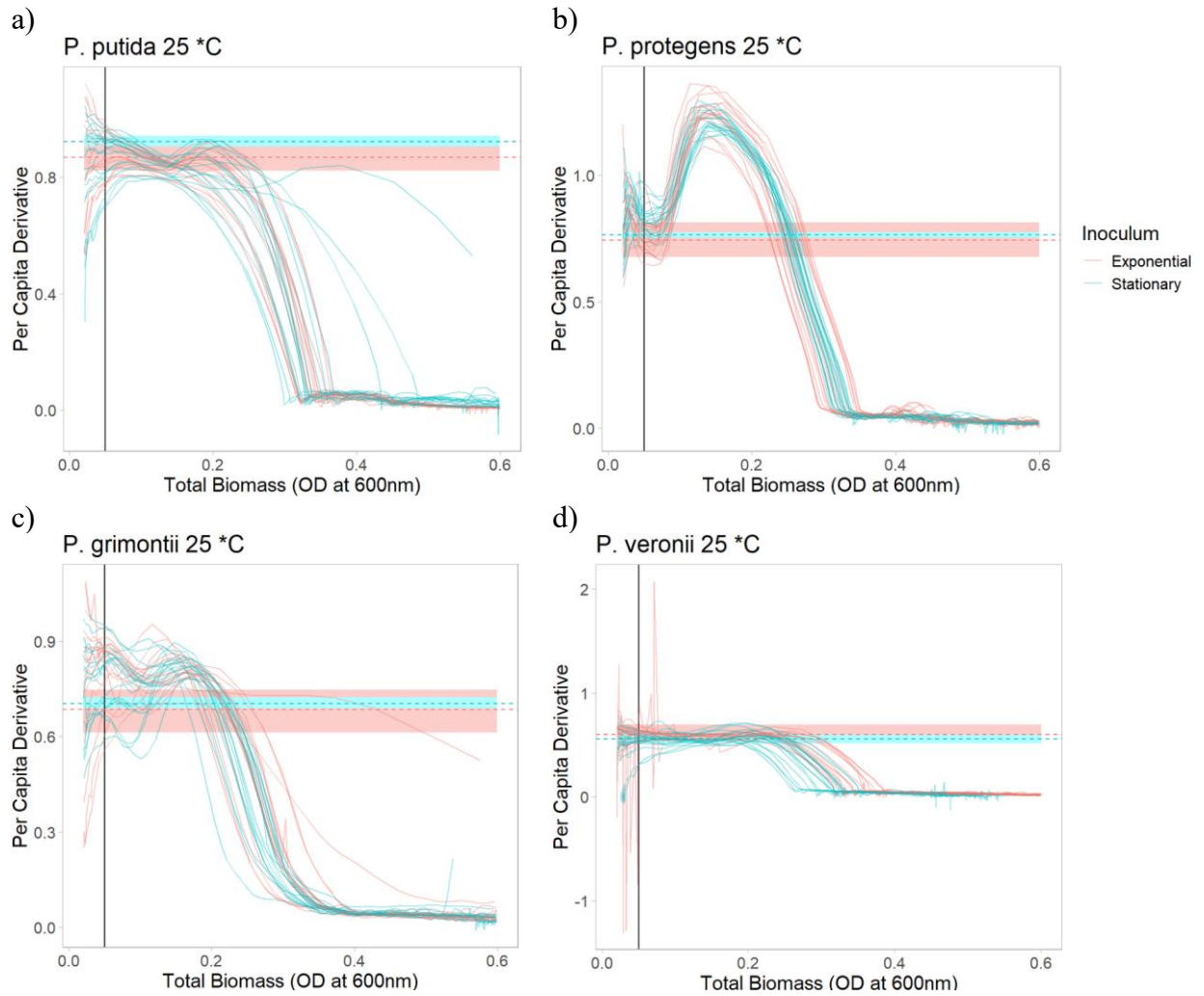
Figure S7. *P. protegens* **(b) exhibits a consistent and strong density-dependence of growth rate at 25°C, as compared to other species (a, c, d).** Each panel shows the per capita derivative of OD (y-axis) as a function of OD (x-axis) at 25°C for batch cultures inoculated at different starting dilutions from either early exponential (red) or stationary (blue) phase. The horizontal dashed lines show the mean of the intrinsic growth rate, coloured by exponential or stationary phase estimate, and the ribbons show the corresponding 95% confidence intervals. The black vertical line shows the threshold of detection that was used to estimate the intrinsic growth rate. By convention, the intrinsic growth rate (μ) is defined as the growth rate in the absence of density-dependent effects. For all species, the intrinsic growth rate estimates are in good agreement with the per capita derivatives at low density (i.e., near the black line). **b)** *P. protegens* cultures show a consistent ~50% increase in the per capita derivative of OD at intermediate OD (~0.15) as compared to low OD. This could suggest that *P. protegens* cells can facilitate each other's growth more than other species.

Table S2. Non-parametric tests of whether intrinsic growth rate rank at ambient temperatures is correlated with that at extreme heat (Spearman's rank correlation).

Correlation of species rank at 25°C with that at 40°C

rho = -0.34	S = 46.8	p-value = 0.51

Correlation of species rank at 30°C with that at 40°C

rho = 0.30	S = 24.4	p-value = 0.56

Table S3. Parametric tests of whether intrinsic growth rate at ambient temperatures is correlated with that at extreme heat (linear mixed effects model).

lm(intrinsic growth rate at 40°C ~ intrinsic growth rate at 25°C + (1 | Species))

Efron R^2 = 0.962

	Estimate	SE	p-value
Fixed effects			
Intercept	0.084	0.13	0.52 (NS)
Growth at 25°C	0.068	0.14	0.63 (NS)
Random effect			
Species (intercept)	0.037	0.19	

lm(intrinsic growth rate at 40°C ~ intrinsic growth rate at 30°C + (1 | Species))

Efron R^2 = 0.962

	Estimate	SE	p-value
Fixed effects			
Intercept	0.21	0.20	0.28 (NS)
Growth at 30°C	-0.086	0.20	0.67 (NS)
Random effect			
Species (intercept)	0.038	0.19	

Table S4. Parametric test of whether intrinsic growth rate at ambient temperatures is correlated with the relative growth by CFU (linear mixed effects model).
Bonferroni-corrected α = 0.025

lm(relative growth by CFU at 40°C ~ intrinsic growth rate at 25°C + (1 | Species))

Efron R^2 = 0.81

	Estimate	SE	p-value
Fixed effects			
Intercept	0.26	0.49	0.59 (NS)
Growth at 25°C	0.034	0.60	0.96 (NS)
Random effect			
Species (intercept)	0.15	0.38	

lm(relative growth by CFU at 40°C ~ intrinsic growth rate at 30°C + (1 | Species))

Efron R^2 = 0.83

|	Estimate	SE	p-value
Fixed effects			
Intercept	-0.98	0.66	0.14 (NS)
Growth at 30°C	1.4	0.70	0.048 (NS)
Random effect			
Species (intercept)	0.13	0.36	

Results for Experiment II
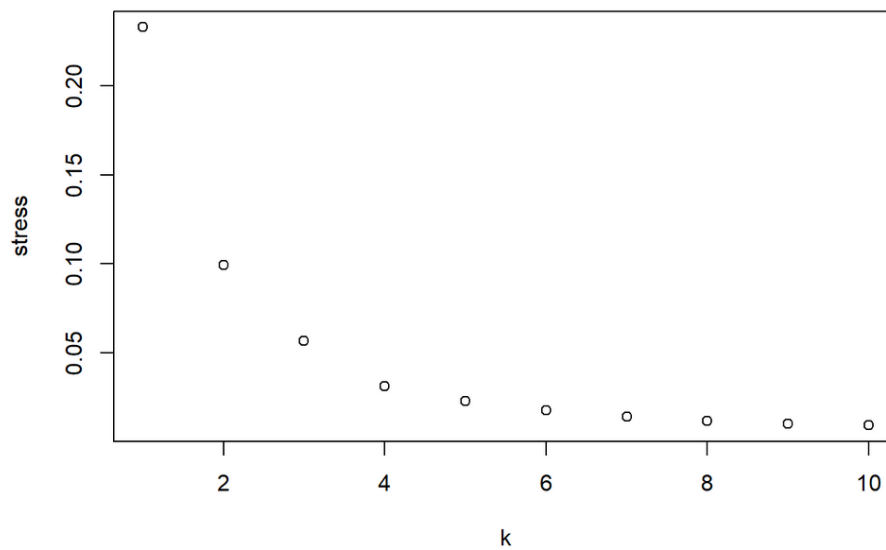
Figure S8. Scree plot of NMDS ordination for all communities over time on the resistance, early recovery, and late recovery days. Three dimensions were used for the analysis as the this is dimensionality is readily interpretable and the decrease in stress plateaus off around k=3.
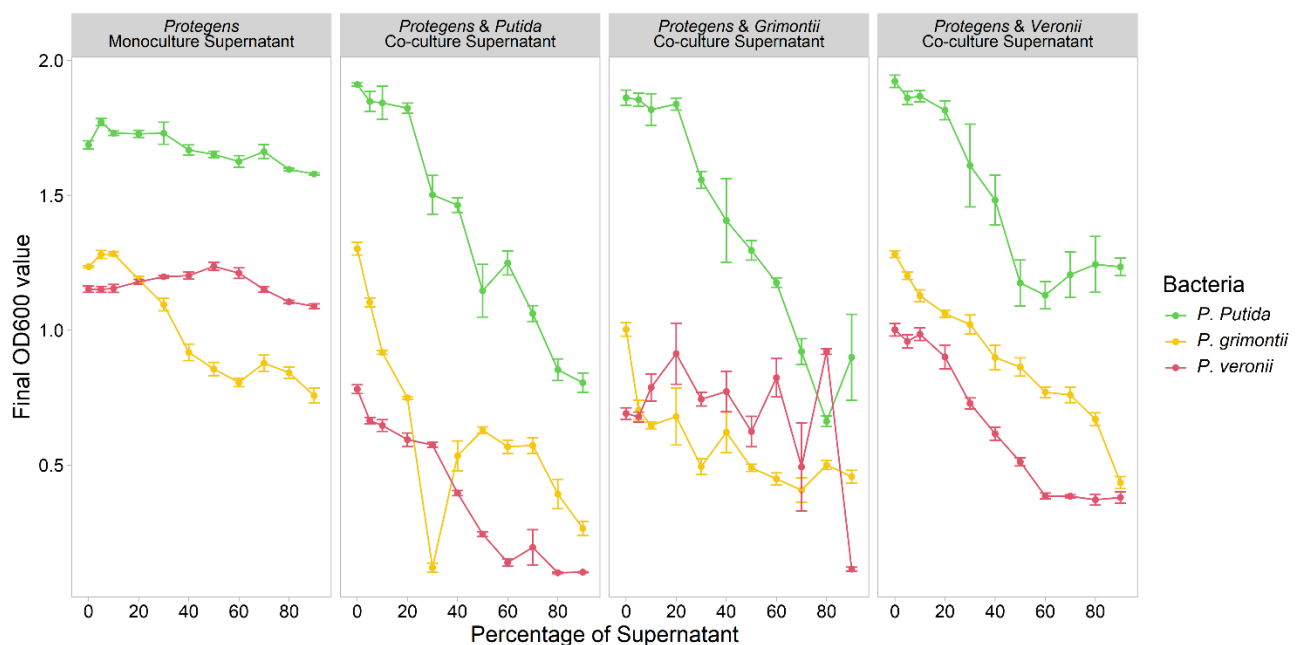
**Figure S9. Average OD values for three of the focal species after 12 hours of growth versus percentage of media that is supernatant (compared to fresh 50% LB).** This figure is the same style and is part of the motivation for Figure 3C. Here we compare the growth of these bacterial species when subjected to *P. protegens* supernatant when *P. protegens* is grown alone versus when *P. protegens* is grown with another species.
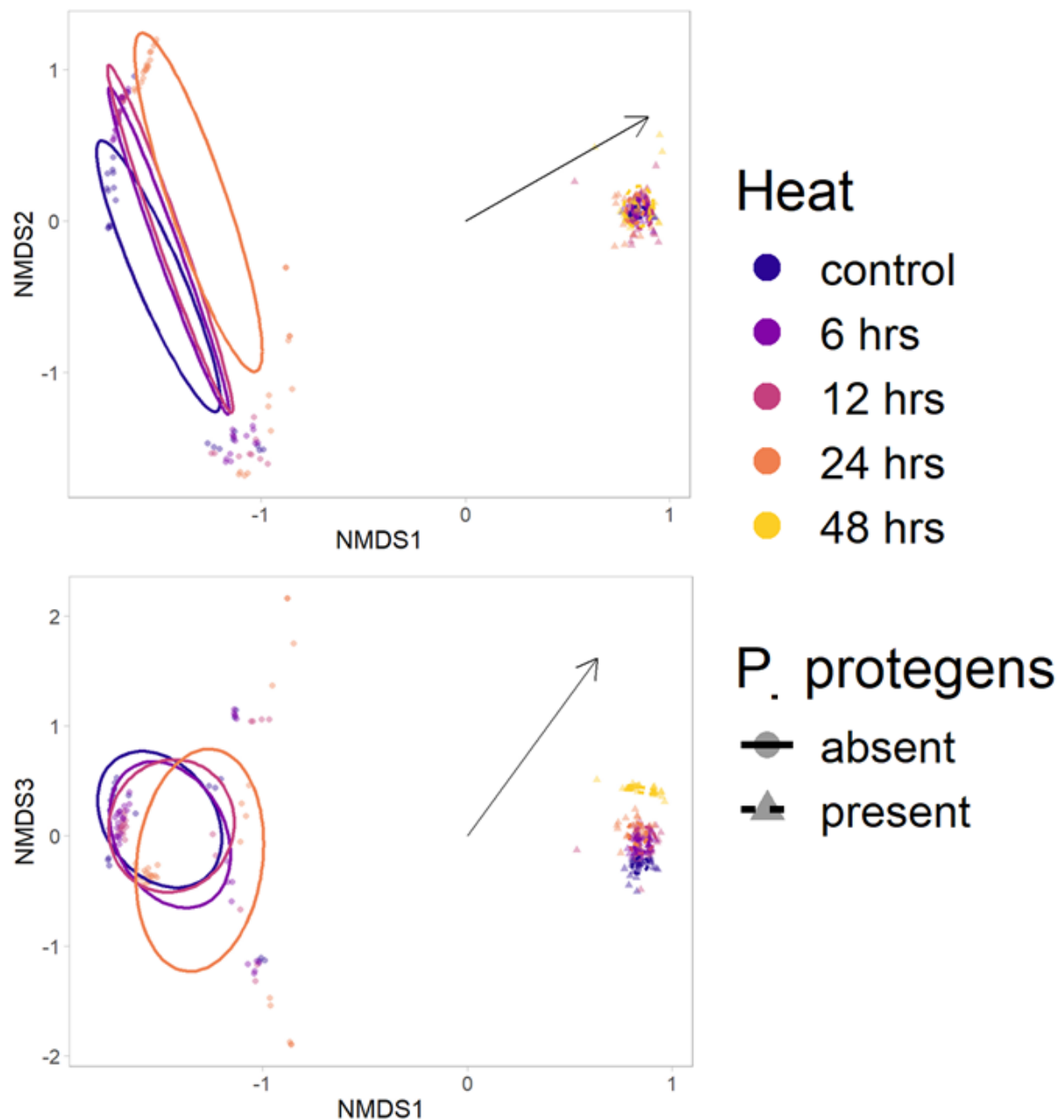
Figure S10. NMDS ordination for the data excluding the communities without *P. protegens* that were exposed to 48h heat pulse duration. The figure style is the same as Figure 3A from the main text except for the thin black arrows. The arrows show the direction of the environmental gradient of heat pulse duration (which is statistically significant, p<0.001).
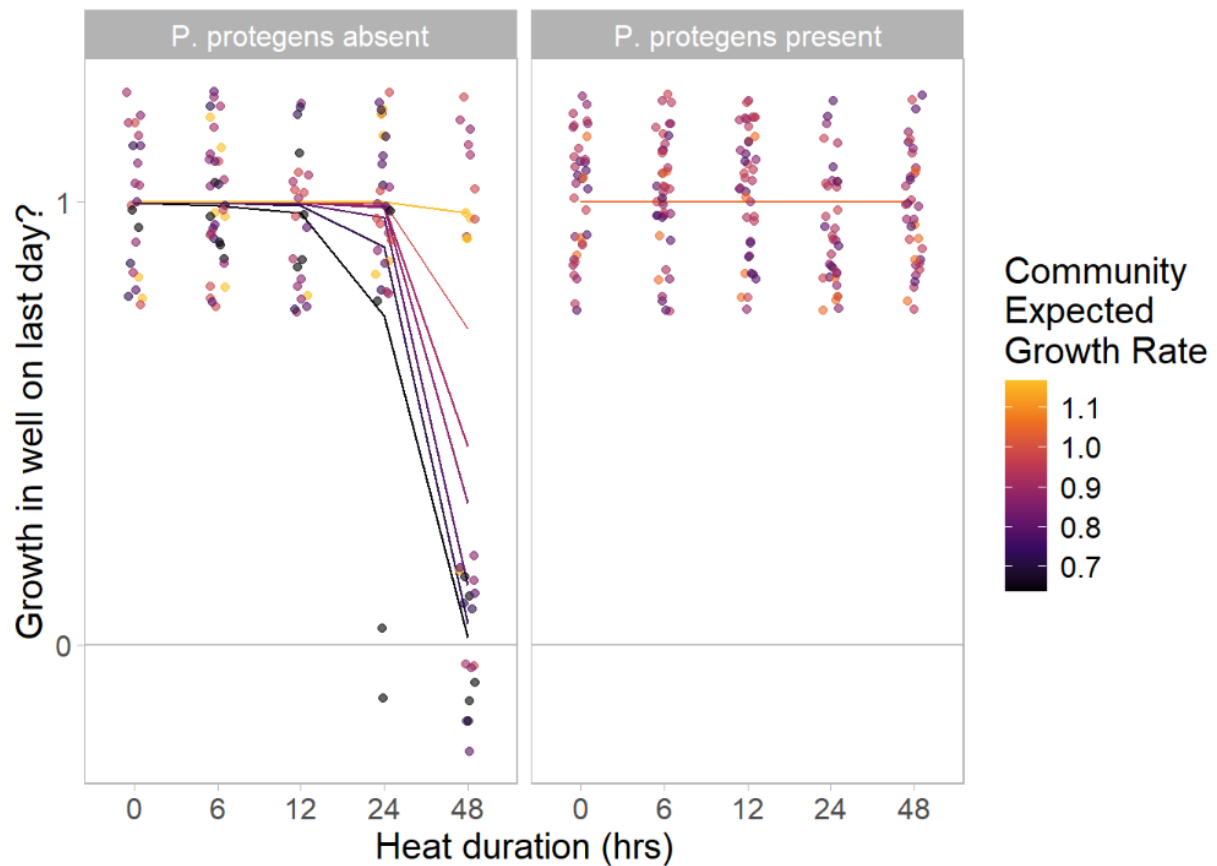
Figure S11. Logistic regression found three risk factors for community extinction: the duration of the heat pulse, the absence of *P. protegens* from the community, and slow community expected growth rate. Points show the observed data and lines show the logistic model predictions. Heat duration was treated as a numeric variable in the model although it is shown here on the x-axis as a categorical variable. The y-axis is binary and indicates whether growth was observed in the well two days after the end of the heat pulse (i.e., the final day of the experiment). Colours show the community expected growth rates, and the facets show communities without (left) and with (right) *P. protegens*. Multiple identical model predictions are stacked on top of one another in the right facet.
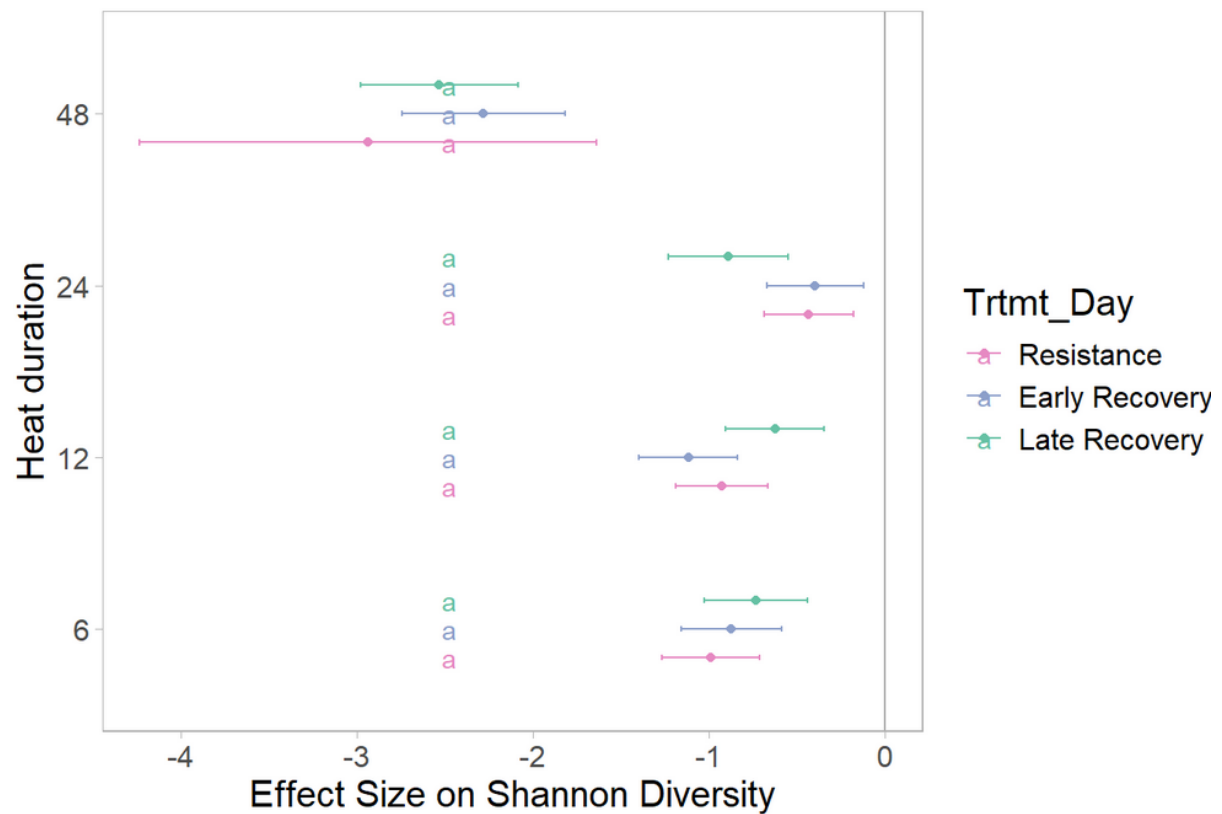
Figure S12. Forest plot of the effect sizes on Shannon diversity for the complete data (i.e., *including* communities that went extinct). The figure style is the same as Figure 4A from the main text. The colours indicate different treatment days and the letters indicate treatment days *within the same heat pulse duration* that are statistically indistinguishable.

Table S5. Pairwise t-tests between heat pulse durations on the effect sizes of Shannon diversity for the complete data (i.e., *including* communities that went extinct). Bonferroni-corrected α = 0.001

Treatment Day	1st Heat Pulse Duration	Compared to 2nd Heat Pulse Duration	t-statistic	df	p-value	Adjusted p-value	
Resistance	6 hrs	12 hrs	-1.17	24.2	0.253	1.00	NS
		24 hrs	-10.3	23.2	$p < 10^{-9}$	$p < 10^{-6}$	*
		48 hrs	9.79	11.3	$p < 10^{-6}$	$p < 10^{-4}$	*
	12 hrs	24 hrs	-9.25	22.5	$p < 10^{-6}$	$p < 10^{-6}$	*
		48 hrs	10.1	11.3	$p < 10^{-6}$	$p < 10^{-4}$	*
	24 hrs	48 hrs	12.6	11.3	$p < 10^{-6}$	$p < 10^{-6}$	*
Early Recovery	6 hrs	12 hrs	4.32	24.2	$p < 10^{-3}$	0.00418	NS
		24 hrs	-8.38	23.0	$p < 10^{-6}$	$p < 10^{-6}$	*
		48 hrs	17.5	16.8	$p < 10^{-9}$	$p < 10^{-9}$	*
	12 hrs	24 hrs	-12.6	22.4	$p < 10^{-9}$	$p < 10^{-9}$	*
		48 hrs	14.5	16.9	$p < 10^{-9}$	$p < 10^{-6}$	*
	24 hrs	48 hrs	23.3	17.0	$p < 10^{-12}$	$p < 10^{-12}$	*
Late Recovery	6 hrs	12 hrs	-1.93	24.2	0.0655	1.00	NS
		24 hrs	2.37	21.5	0.0274	0.493	NS
		48 hrs	22.8	17.7	$p < 10^{-12}$	$p < 10^{-12}$	*
	12 hrs	24 hrs	4.10	20.9	$p < 10^{-3}$	0.00932	NS
		48 hrs	24.4	17.3	$p < 10^{-12}$	$p < 10^{-12}$	*
	24 hrs	48 hrs	19.5	19.6	$p < 10^{-12}$	$p < 10^{-12}$	*
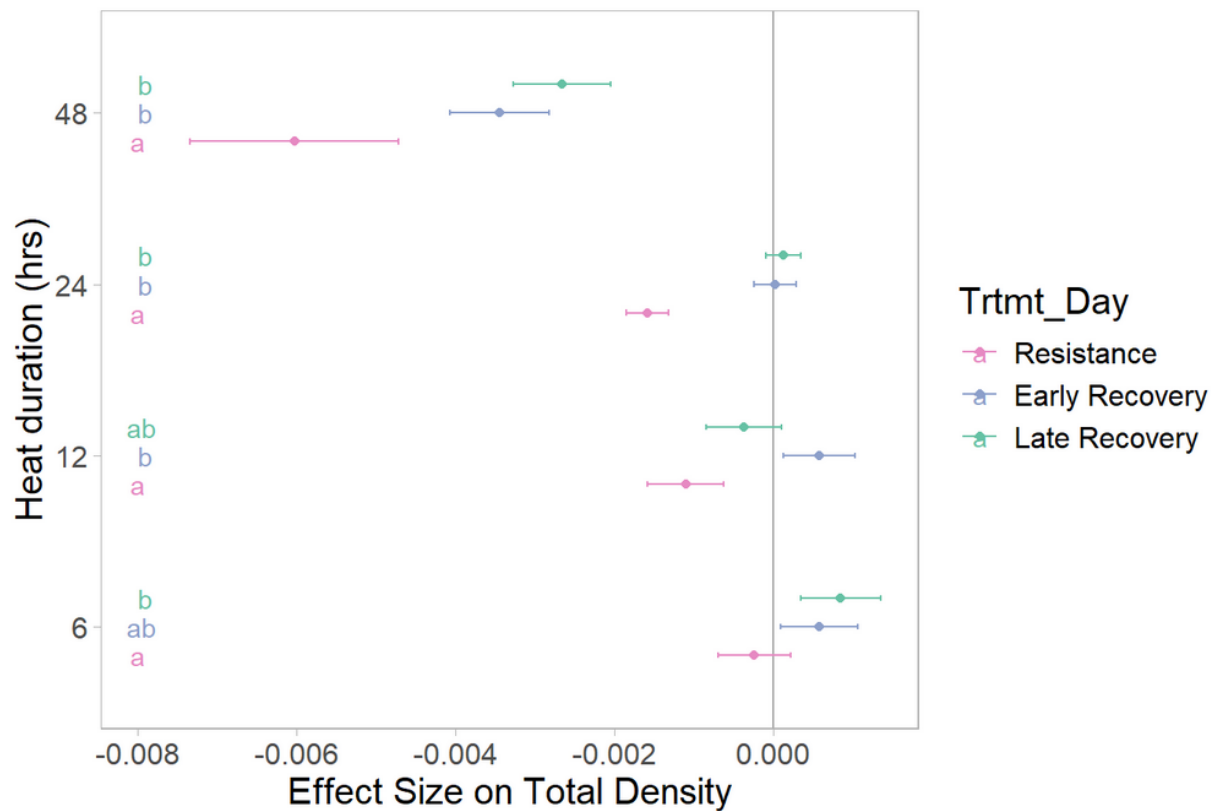
Figure S13. Forest plot of the effect sizes on productivity for the complete data (i.e., including communities that were never able to recover because they went extinct). The figure style is the same as Figure 4B from the main text. The colours indicate different treatment days and the letters indicate groups of treatment days *within the same heat pulse duration* that are statistically indistinguishable.

Table S6. Pairwise t-tests between heat pulse durations on the effect sizes of total productivity for the complete data (i.e., *including* communities that went extinct). Bonferroni-corrected α = 0.001

Treatment Day	1st Heat Pulse Duration	Compared to 2nd Heat Pulse Duration	t-statistic	df	p-value	Adjusted p-value	
Resistance	6 hrs	12 hrs	10.5	30.8	$p < 10^{-9}$	$p < 10^{-9}$	*
		24 hrs	21.2	28.5	$p < 10^{-18}$	$p < 10^{-15}$	*
		48 hrs	32.9	18.1	$p < 10^{-15}$	$p < 10^{-15}$	*
	12 hrs	24 hrs	6.86	22.6	$p < 10^{-6}$	$p < 10^{-4}$	*
		48 hrs	27.6	19.0	$p < 10^{-15}$	$p < 10^{-12}$	*
	24 hrs	48 hrs	26.1	16.2	$p < 10^{-12}$	$p < 10^{-12}$	*
Early Recovery	6 hrs	12 hrs	-0.0725	32.0	0.943	1.00	NS
		24 hrs	8.27	27.6	$p < 10^{-6}$	$p < 10^{-6}$	*
		48 hrs	40.9	28.9	$p < 10^{-18}$	$p < 10^{-18}$	*
	12 hrs	24 hrs	8.34	23.6	$p < 10^{-6}$	$p < 10^{-6}$	*
		48 hrs	40.9	27.3	$p < 10^{-18}$	$p < 10^{-18}$	*
	24 hrs	48 hrs	40.3	20.1	$p < 10^{-18}$	$p < 10^{-18}$	*
Late Recovery	6 hrs	12 hrs	14.2	31.9	$p < 10^{-12}$	$p < 10^{-12}$	*
		24 hrs	10.9	24.2	$p < 10^{-9}$	$p < 10^{-6}$	*
		48 hrs	35.6	29.3	$p < 10^{-18}$	$p < 10^{-18}$	*
	12 hrs	24 hrs	-7.44	20.3	$p < 10^{-6}$	$p < 10^{-4}$	*
		48 hrs	23.0	28.3	$p < 10^{-18}$	$p < 10^{-18}$	*
	24 hrs	48 hrs	33.8	18.6	$p < 10^{-15}$	$p < 10^{-15}$	*
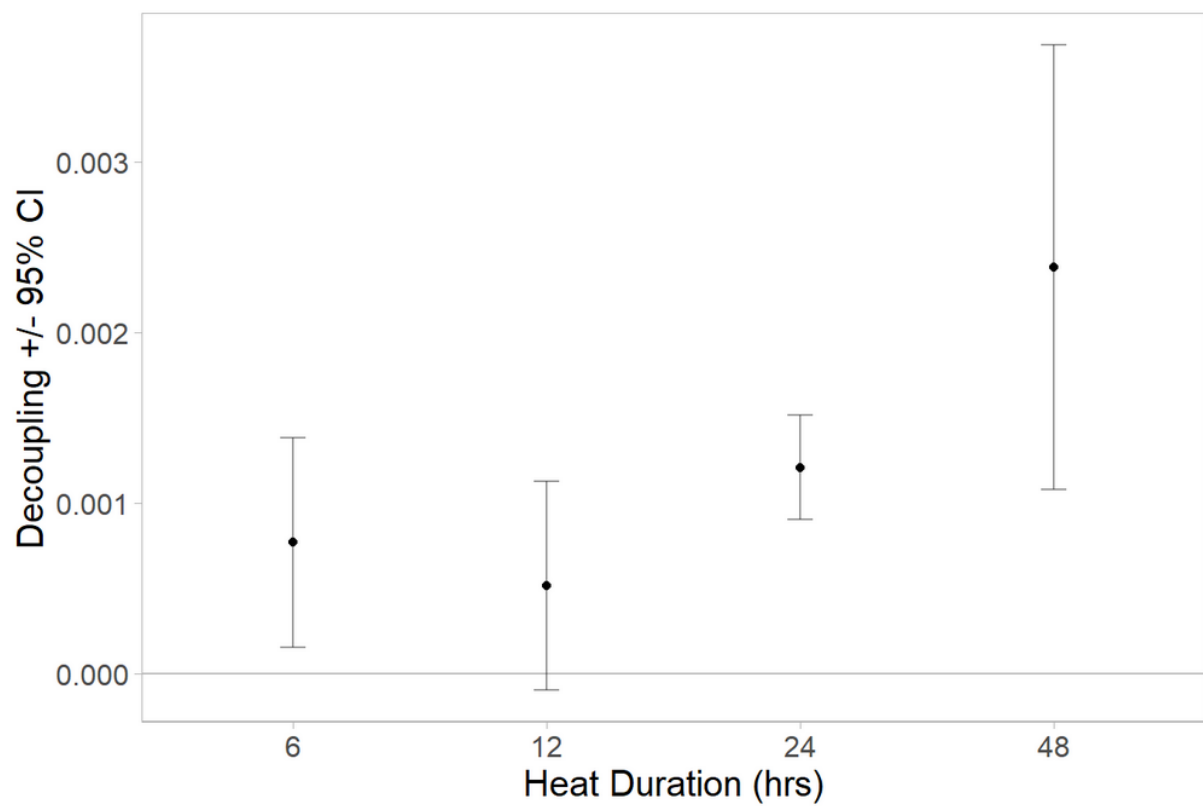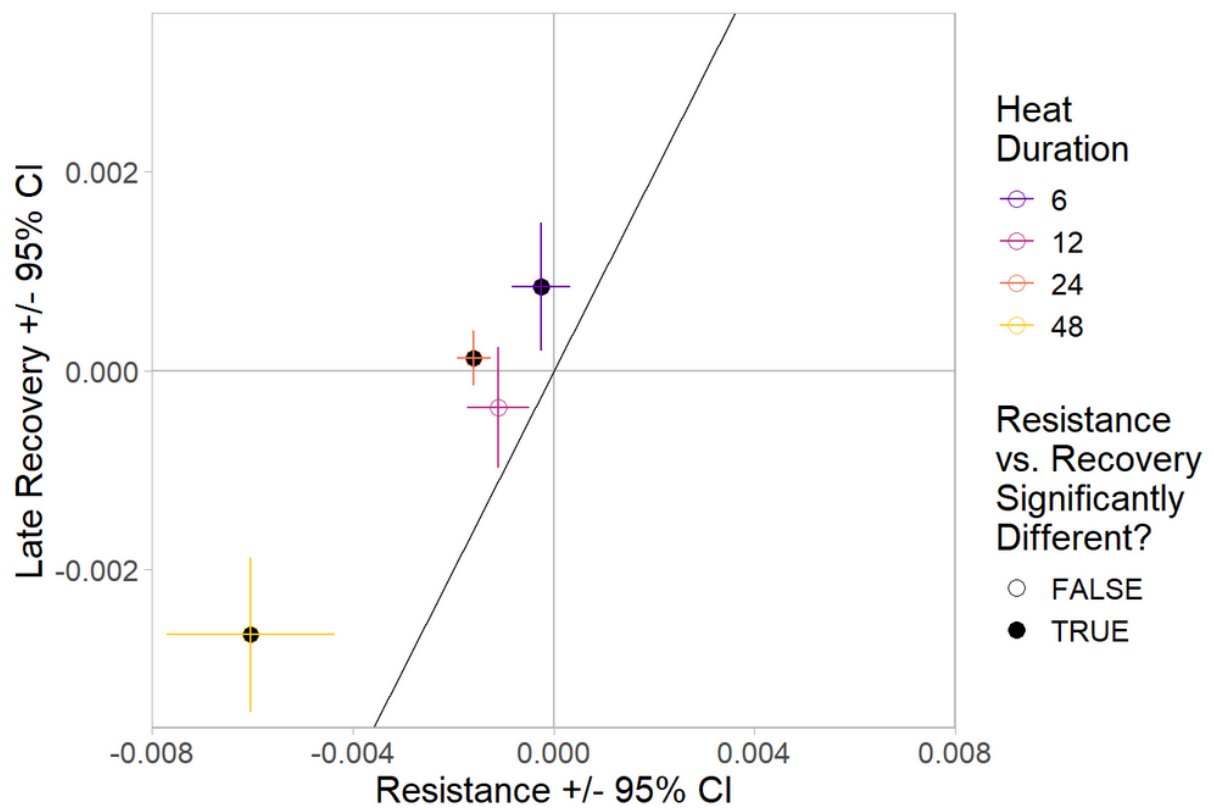
Figure S14. Decoupling plot of the effect sizes on productivity for the completely data (i.e., including communities that went extinct). The figure style is the same as Figure 5 from the main text.